RFID Localization System in Mobile Robotics: A Multi-Hypothesis Kalman Filter Approach with Distributed WLS Algorithm

Elia Bontempelli and Alessandro Rizzardi

***Abstract*—Indoor localization estimation is a research area that has drawn the attention of many scholars in recent years. The key difficulty nowadays is to develop a robust estimating method based on low-cost sensors. A Radio Frequency IDentification (RFID) system is proposed for this purpose, despite the fact that RFID signals can't provide a direct measurement of the distance between the reader and the tag. A Multi-Hypothesis Extended Kalman Filter was used in this study to handle the issue of RFID system phase ambiguity, in order to compute the distance tag-reader and obtain a good localization of the tag in a wide unknown region. In addition, a distributed WLS algorithm is developed to increase estimation performance.**

I. Introduction

Radio Frequency IDentification (RFID) systems have emerged as a pivotal technology in diverse applications, particularly in the fields of item tracking and indoor localization. RFID devices are a preferred choice over alternative technologies with equivalent functionality because to their low cost, low maintenance requirements, and small size. This work focuses on a novel aspect of RFID system deployment in which the tag remains stationary within a somewhat large environment while the mobile robot, on which the reader is mounted, attempts to find and localise it.

The reader sends out an RF signal, which activates passive RFID tags in its vicinity. When an RFID tag receives the reader's signal, it responds by transmitting its data to the reader.

R. Miesen et al. (2011) [1] describe different techniques used to compute the distance between the two devices, such as the received signal strength indicator, the measure of time of arrival or the angle of arrival, or the measurement of the phase of the backscattered signal. The latter technology is the one used for this project.

Despite their prevalence and utility, RFID systems encounter challenges, especially when deployed in environments where precise localization is crucial. Phase-based techniques suffer from ambiguities in distance (location) estimation. Distances which differ by a multiple of $\lambda/2$ (where λ is the wavelength of the signal), give rise to the same phase reading. This ambiguity in the phase measurement make impossible to directly recover the distance between the tag and the reader.

In addressing the challenge at hand, a Multi-Hypothesis Extended Kalman Filter is implemented, similar to the one presented by E. DiGiampaolo and F. Martinelli [3]. The basic idea is to exploit the functionalities of the Kalman Filter, fusing the wheel encoder readings with the RFID signals and then create a certain number of EKF instances, each one initialized on a different cycle corresponding to the initial phase measurement. Ultimately, one of these different instances is selected, associated with an estimate of the distance between the robot and the tag. Actually the approach, while estimating the tag-reader distance, allows to obtain also the bearing of the tag with respect to the reader, i.e., it allows to estimate the relative position of the tag with respect to the robot.

In the second phase of the project, the approach involves tackling the issue in a distributed fashion, with the primary objective of enhancing tag localization precision. The RFID readers are mounted on multiple robots, and that each exchanges information with the others about its own estimate via a distributed WLS algorithm.

The paper is organized as follows: Section II introduces the system and how it is formulated the problem, in Section III is described the proposed solution, that is explained numerically in Section IV. Finally in Section V and VI present the analysis of the results and some final considerations.

II. Adopted Models

The algorithm proposed for this research utilizes a mobile robot equipped with an RFID reader. To conduct a comprehensive simulation, a model has been developed for the robot, that includes the measurements received from the wheel encoders and the signals measured by the reader.

A. Differential Drive Robot Model

The agent used in the tag's research has been chosen to be a mobile robot based on the differential drive model.

The continuous-time model of the robot is described by equations:

$$\begin{aligned} \dot{x} &= v\,cos(\theta) \\ \dot{y} &= v\,sin(\theta) \\ \dot{\theta} &= \omega \end{aligned} \tag{1}$$

where x, y, θ are the variables describing the pose of the robot and v, ω are respectively the linear velocity and the changing rate of the robot orientation.

In order to proceed with the simulation, the Euler method is used to discretize the systems in Eqs. 1, resulting in:

$$\begin{aligned} x_{k+1} &= x_k + v_k\, cos(\theta_k)\, \Delta t \\ y_{k+1} &= y_k + v_k\, sin(\theta_k)\, \Delta t \\ \theta_{k+1} &= \theta_k + \omega\, \Delta t \end{aligned} \tag{2}$$

where Δt is the integration step.

It is possible to find also a relation between v, ω and the angular velocities of the wheels ω_R, ω_L as shown in Eq. 3.

$$\begin{pmatrix} v \\ \omega \end{pmatrix} = R \begin{pmatrix} 1/2 & 1/2 \\ 1/d & 1/d \end{pmatrix} \begin{pmatrix} \omega_R \\ \omega_L \end{pmatrix} \tag{3}$$

where R is the wheels radius and d is the distance between the wheels.

B. Odometry Model

The encoders readings of the robot are related to the wheels displacement so the measurement of the robot system has been modeled as:

$$\begin{aligned} \hat{u}_R &= u_R + \eta_R \\ \hat{u}_R &= u_R + \eta_R \end{aligned} \tag{4}$$

where the noise terms are 0-mean Gaussian random variables with variance:

$$\begin{aligned} \sigma_R^2 &= K_R\, |u_R| \\ \sigma_L^2 &= K_L\, |u_L| \end{aligned} \tag{5}$$

The variance is computed as a value proportional to the actual displacement scaled by constant factors K_R and K_L. The model of this measurement system has been used in the development of the odometry model.

Considering the Eq. 3, an approximation for the wheel velocities can be derived as presented in Eq. 6.

$$\begin{aligned} \omega_R &= \frac{d}{dt}\phi_R \simeq \frac{\Delta\phi_R}{\Delta t} \\ \omega_R &= \frac{d}{dt}\phi_R \simeq \frac{\Delta\phi_R}{\Delta t} \end{aligned} \tag{6}$$

where $\Delta\phi_R$, $\Delta\phi_L$ are the angular displacement of the wheels.

By substituing Eq. 6 in the discrete model described in Eq. 2, the resulting system can be expressed as follows:

$$\begin{aligned} x_{k+1} &= x_k + \frac{R}{2}\left(\Delta\phi_R + \Delta\phi_L\right) cos(\theta_k) \\ y_{k+1} &= y_k + \frac{R}{2}\left(\Delta\phi_R + \Delta\phi_L\right) sin(\theta_k) \\ \theta_{k+1} &= \theta_k + \frac{R}{d}\left(\Delta\phi_R + \Delta\phi_L\right) \end{aligned} \tag{7}$$

The displacement of the wheels can be written as:

$$\begin{aligned} u_L &= R\, \Delta\phi_L \\ u_R &= R\, \Delta\phi_R \end{aligned} \tag{8}$$

Considering a measurement of these quantities as described in Eq. 4, the model of the odometry estimation is built as written below:

$$\begin{aligned} \hat{x}_{k+1} &= \hat{x}_k + \frac{1}{2}\left(\hat{u}_{R,k} + \hat{u}_{L,k}\right) cos(\theta_k) \\ \hat{y}_{k+1} &= \hat{y}_k + \frac{1}{2}\left(\hat{u}_{R,k} + \hat{u}_{L,k}\right) sin(\theta_k) \\ \theta_{k+1} &= \hat{\theta_k} + \frac{1}{d}\left(\hat{u}_{R,k} - \hat{u}_{L,k}\right) \end{aligned} \tag{9}$$

That can be simplified considering:

$$\begin{aligned} \hat{u}_k &= \frac{\hat{u}_{R,k} + \hat{u}_{L,k}}{2} \\ \hat{\omega}_k &= \frac{\hat{u}_{R,k} - \hat{u}_{L,k}}{d} \end{aligned} \tag{10}$$

Therefore the final pose estimation of the robot can be suppose in Eq. 11.

$$\begin{aligned} \hat{x}_{k+1} &= \hat{x}_k + \hat{u}_k\, cos(\theta_k) \\ \hat{y}_{k+1} &= \hat{y}_k + \hat{u}_k\, sin(\theta_k) \\ \theta_{k+1} &= \hat{\theta_k} + \hat{\omega}_k \end{aligned} \tag{11}$$

C. RFID Model

The Radio-Frequency Identification (RFID) is a technology that uses radio waves to transfer data between two main components: the RFID tag and the RFID reader.

The reader has an antenna that emits radio frequency signals while tag has one that is responsible for receiving and transmitting back the radio frequency signal, often the tag is passive and only activate when receiving the signal from the reader.

When a tag enters in the range of the reader, the reader sends out a signal. The tag, upon receiving the signal, is powered by the energy from the incoming radio waves. The powered tag then transmits back to the reader. The reader receives the signal and it is able to measure the phase difference between the signal sent and received.

Given a signal with frequency f, the phase of this signal over time is computed as:

$$\varphi = \omega \cdot t \tag{12}$$

where $\omega = 2\pi f$.

In this project the model of the phase measurement at time step k, is considered as:

$$\varphi = mod\left(-\frac{4\pi}{\lambda} \cdot \rho_k + \eta_{\varphi,k}, 2\pi\right) \tag{13}$$

, where λ is the wavelength of the electromagnetic signal, ρ_k is the unknown tag-reader distance and η_φ is 0-mean Gaussian noise, i.e., $\eta_\varphi \sim \mathcal{N}(0, \sigma_\varphi^2)$.

Supposing the signal travels from the reader to the tag and back, the distance between them will be:

$$d = \frac{1}{2}\, c \cdot t_f \tag{14}$$

with c the speed of light and t_f the time of flight.

Therefore, the distance between the tag and the reader can be expressed as:

$$d = \frac{1}{2}\, c\, \frac{\varphi}{\omega} = \frac{1}{2}\, \frac{c\,\varphi}{2\pi f} = \frac{1}{2}\, \frac{\lambda}{2\pi}\, (2n\pi + \varphi) \tag{15}$$

The primary challenge encountered is that the reader can solely measure φ, making it impossible to directly retrieve the number of wavelengths (n). Consequently, this limitation makes determining the exact distance between the tag and the reader difficult.

III. Solution Approach

A. Tag position identification with MHEKF

The robot-tag distance ρ and the bearing angle β are the two parameters utilized to identify the tag position in relation to the robot position.

$$\rho = \sqrt{(x_r - x_T)^2 + (y_r - y_T)^2} \tag{16}$$

$$\beta = \theta_r - \text{atan2}(y_T - y_r, x_T - x_r) \tag{17}$$

After discretization, it is possible to write the dynamics of the variables ρ_k and β_k as functions of the wheel displacements $u_{R,k}$ and $u_{L,k}$:

$$\rho_{k+1} = \rho_k - u_k\, \cos(\beta_k) \tag{18}$$

$$\beta_{k+1} = \beta_k + \omega_k + \frac{u_k}{\rho_k}\, \sin(\beta_k) \tag{19}$$

The objective is to retrieve the tag position using simply encoder reading and RFID signal phase measurements. A proposed solution is the implementation of a Kalman Filter to directly estimate the system state $\xi = (\rho_k \quad \beta_k \quad x_k \quad y_k \quad \theta_k)^T$ of our system.

The measurement model can be considered as follows:

$$z_k = \begin{pmatrix} 1 & 0 & 0 & 0 & 0 \end{pmatrix} \xi + \eta_k \tag{20}$$

As highlighted in Section II, a significant challenge is the inability to directly measure the range ρ, due to phase ambiguity. To address this issue, multiple Kalman filters are concurrently run, each initiated with a distinct initial condition based on the signal's wavelength. Assuming knowledge of the maximum range ρ_{max} at which the reader can detect the tag, each phase measurement could correspond to one of $n_{max} = \rho_{max} \cdot \lambda/2$ possible different distances between the robot and the tag. Consequently, several Kalman filters are employed to evaluate all these different hypotheses (MHEKF).

The following steps, representing the procedure employed, are applicable to every EKF instance.

1) Initialization: The filter is initialized as soon as a phase measurement is available. Let the initial state of the Extended Kalman Filter be as follows:

$$\hat{\rho}_0 = -\frac{1}{4\pi}\lambda\, \hat{\varphi} + n\, \frac{\lambda}{2} \quad n = 1, \ldots, n_{max} \tag{21}$$

$$\hat{\beta} = 0 \tag{22}$$

$$\hat{x}_0 = x_i \tag{23}$$

$$\hat{y}_0 = y_i \tag{24}$$

$$\hat{\theta}_0 = \theta_i \tag{25}$$

and the initial covariance matrix of the estimate:

$$P_0 = \begin{pmatrix} \sigma_\rho^2 & 0 & 0 & 0 & 0 \\ 0 & (\pi/3)^2 & 0 & 0 & 0 \\ 0 & 0 & cov(x_i^2) & cov(x_i\, y_i) & cov(x_i\, \theta_i) \\ 0 & 0 & cov(y_i\, x_i) & cov(y_i^2) & cov(y_i\, \theta_i) \\ 0 & 0 & cov(\theta_i\, x_i) & cov(\theta_i\, y_i) & cov(\theta_i^2) \end{pmatrix} \tag{26}$$

2) Prediction Step:

$$\hat{\rho}^-_{k+1} = \hat{\rho}_k - \hat{u}_k\, \cos(\beta_k) \tag{27}$$

$$\hat{\beta}^-_{k+1} = \hat{\beta}_k + \hat{\omega}_k + \frac{\hat{u}_k}{\rho_k}\, \sin(\beta_k) \tag{28}$$

$$\hat{x}^-_{k+1} = \hat{x}_k + \frac{1}{2}\, \hat{u}_k\, cos(\theta_k) \tag{29}$$

$$\hat{y}^-_{k+1} = \hat{y}_k + \frac{1}{2}\, \hat{u}_k\, sin(\theta_k) \tag{30}$$

$$\hat{\theta}^-_{k+1} = \hat{\theta}_k + \frac{1}{d}\, \hat{\omega}_k \tag{31}$$

$$P^-_{k+1} = F_k\, P_k\, F_k^T + W_k\, Q_k\, W_k^T \tag{32}$$

where F and W are the Jacobian matrix of the state dynamics (see Section VII).

3) Correction Step: Let $z_{k+1} = \varphi_{k+1} + \eta_\rho$ be the measurement available at time step $k+1$, the innovation term is given by $\varphi_{k+1} - \hat{\varphi}_{k+1}$, where

$$\hat{\varphi}_{k+1} = mod(-\frac{4\pi}{\lambda} \cdot \hat{\rho}_{k+1}, 2\pi)$$

is the expected phase measurement at this stage. Therefore, the correction step, for the state and the covariance matrix, is respectively:

$$\hat{\xi}_{k+1} = \hat{\xi}^-_{k+1} + K_{k+1}\, (\varphi_{k+1} - \hat{\varphi}_{k+1}) \tag{33}$$

$$P_{k+1} = (I - K_{k+1}\, H)\, P^-_{k+1} \tag{34}$$

where:

$$K_{k+1} = P^-_{k+1}\, H^T\, (H\, P^-_{k+1}\, H^T + \sigma_\rho^2)^{-1} \tag{35}$$

is the Kalman gain and the Jacobian matrix H is given by:

$$H = \left(-\frac{4\pi}{\lambda}, 0, 0, 0, 0 \right)$$

4) Weighing EKF instances: Every instance need to be weighed in order to find a criteria for selecting the one that gives us the best estimate.

The weight is initialized for all instances as:

$$w_i = \frac{1}{n_{max}} \quad i = 1, \ldots, n_{max}$$

and at every steps is computed as follows:

$$w_i = w_i\, e^{-\frac{1}{2}\, (H\, P\, H^T + \sigma_\phi)^{-1}\, (\varphi - \hat{\varphi})^2}$$

The formula above represents the Gaussian random variable innovation's probability density function with variance $(H\, P\, H^T + \sigma_\varphi)$, where σ_φ^2 is the variance over the phase measurement and follow the relation $\sigma_\rho = \sigma_\varphi\, \lambda/(4\pi)$.

B. Distributed Algorithm

To improve the estimation of an individual robot, a distributed approach is employed. The idea is to implement the distributed WLS algorithm in which each node (robot) transmits its information to all the other nodes in its communication range. Under some mild connectivity properties all the nodes in the network will have all the data in the network. Finally each node can solve the WLS and hence each node has the same best LS solution.

Each node can compute a measurement of the tag position:

$$z = \begin{pmatrix} 1 & 0 \\ 0 & 1 \end{pmatrix} \begin{pmatrix} x_T \\ y_T \end{pmatrix} + \eta_T \tag{36}$$

Each robot computes the estimate of the tag position as:

$$\hat{x}_T = \hat{x}_R + \hat{\rho}\,\cos(\hat{\theta}_R - \hat{\beta})$$
$$\hat{y}_T = \hat{y}_R + \hat{\rho}\,\sin(\hat{\theta}_R - \hat{\beta})$$

where $(\hat{\rho}, \hat{\beta}, \hat{x}_R, \hat{y}_R, \hat{\theta}_R)$ is the state of the selected EKF instance, at every step.

The covariance matrix of the estimation error is defined as:

$$Cov(\eta_T) = J\,P\,J^T \tag{37}$$

where P is the covariance matrix of the state $\xi = (\rho, \beta, x_R, y_R, \theta)$, while J is the Jacobian matrix of the position of the tag referred to the state ξ:

$$J = \begin{pmatrix} \cos(\hat{\theta} - \hat{\beta}) & \hat{\rho}\,\sin((\hat{\theta} - \hat{\beta})) & 1 & 0 & -\hat{\rho}\,\sin(\hat{\theta} - \hat{\beta}) \\ \sin(\hat{\theta} - \hat{\beta}) & -\hat{\rho}\,\cos(\hat{\theta} - \hat{\beta}) & 0 & 1 & \hat{\rho}\,\cos(\hat{\theta} - \hat{\beta}) \end{pmatrix} \tag{38}$$

The global WLS solution for each robot is computed as:

$$\begin{pmatrix} \hat{x}_T \\ \hat{y}_T \end{pmatrix} = F_i^{-1}\,a_i \tag{39}$$

where F_i and a_i are respectively the local composite information matrix and the local composite information state, for each node:

$$F_i = H\,Cov(\eta_T)^{-1}\,H^T$$
$$a_i = H^T Cov(\eta_T)\,\begin{pmatrix} \hat{x}_{i,T} \\ \hat{y}_{i,T} \end{pmatrix}$$

Applying an average consensus algorithm involves exchanging a significant number of messages between nodes. This process ensures that, at a steady state, all estimates converge to a common global Weighted Least Squares (WLS) solution, achieving a consensus equilibrium.

The exchange of messages is based on a network structure given by an adjacency matrix built considering random connections of the robots inside the tag range. In particular, the updating rule for the average consensus used in this research, is based on the *maximum-degree weight* of the adjacency matrix and it is the following:

$$F_i(k+1) = F_i(k) + \sum_{j=1}^{n} \frac{1}{1 + d_{max}}(F_j(k) - F_i(k))$$
$$a_i(k+1) = a_i(k) + \sum_{j=1}^{n} \frac{1}{1 + d_{max}}(a_j(k) - a_i(k))$$

So, finally, we will have that:

$$\begin{pmatrix} \hat{x}_T \\ \hat{y}_T \end{pmatrix} = \lim_{k \to \infty} F_i(k)^{-1}\,a_i(k) \tag{40}$$

IV. Implementation Details

A series of simulations have been carried out to demonstrate the accuracy of the algorithm.

A $100\,m^2$ room was employed as the simulation's environment. In this setting, the mobile robots indicated in Eq.2 move around looking for the tag.

The distance between the wheels d has been set to $50cm$, while it has been chosen $20cm$ for the radius of the wheels R.

The environment has been built up so that the tag position in unknown by the robots, but their initial positions is assumed to be known by themselves. The robots search randomly around the map, generating random target points. If one of the robot finds the tag while it is within the range of the RFID signal, it sends its location to the other robot, which immediately points to the communicated location.

The RFID signal has been set to have a frequency of $867 \cdot 10^6\,Hz$, meaning a wavelength around $35\,cm$. The signal range has been set to $2m$, meaning that every robot has to compute 12 Kalman filters to determine in which cycle is the tag.

As previously indicated in Section II the noise incorporated into the phase measurement, denoted as η_φ, is a 0-mean Gaussian noise with standard deviation σ_φ. The numerical investigations performed mainly consider $\sigma_\varphi = 0.2\,rad = 11.5°$, however, further investigations with different values have been performed.

In the context of robot odometry model, the constants K_R and K_L in Eq. 5, when multiplied by the length of the robot's position displacement, produce the variance of the odometry inaccuracy. For instance, if the robot travels a 10-meter path and the constants are set to 0.001, it implies an error of 0.1 meters, corresponding to a variance of 0.01 m^2. It's important to note that these values are influenced solely by the precision of the encoder sensors and they could be determined through calibration procedures.

In the majority of the experiments, the constant are set to be $K_R = K_L = 0.01 \cdot 10^-3$ that correspond to an error of 1 cm along 10-meter path. In other tests different values of K_R and K_L are considered, to understand how the estimate changes with different accuracy of the encoder sensors.

The motion of the robots in the environment towards the computed target points, is regulated by a proportional controller, such that:

$$\omega = K_{P,\omega} \cdot e_\theta$$
$$v = K_{P,v} \cdot \delta \tag{41}$$

where:

$$\begin{aligned} \delta &= \sqrt{(y_d - y_R)^2 + (x_d - x_R)^2} \\ e_\theta &= atan\left(\frac{\sin(\theta_d - \theta_R)}{\cos(\theta_d - \theta_R)}\right) \\ \theta_d &= atan\left(\frac{y_d - y_R}{x_d - x_R}\right) \end{aligned} \tag{42}$$

It has been also imposed that the linear velocity v of the robot can not exceed $2m/s$

The distributed algorithm include all the robots inside the range (i.e. all the nodes that have an estimate of the tag position) and it performs the consensus algorithm with an exchange of 50 messages for each iteration.

V. Experimental Results Analysis

A Monte-Carlo analysis was performed in order to obtain a quantitative characterization of the algorithm. Four major tests have been carried out, three of which used a single robot in the environment and one of which examined the performance of the distributed algorithm.

- Test 1: analysis of the general performance of the algorithm
- Test 2: analysis with different encoder errors
- Test 3: analysis with different phase measurement errors
- Test 4: analysis of the distributed algorithm

Test 1 and 4 are performed with fixed values regarding the errors of the sensors of our robot: encoder readings and RFID signal measurements. Instead, the objective of test 2 and 3 was to understand respectively, the incidence of encoder readings error and phase measurement error, on the final estimate of the position of the tag.

A number of 500 trials for all the tests were conducted to gain a clear understanding of the precision and accuracy of the algorithm.

A. Analysis of the general performance of the algorithm

In Table I are reported the parameters used for this test.

Fig. 1 reports the results of a single experiment and it shows that the error converges to zero after a relative small number of iterations, proving the efficiency of the algorithm. While Fig. 2 shows the mean error results of each experiment computed on the last 1500 steps and reports the average mean errors along x, y axis and also the average error over the estimate of the distance from the tag. It's possible to see that, on average, the distance error of the experiments where the estimation is performed by a single robot, is about 7.5 cm.

K_R, K_L	$0.01 * 10^-3$
σ_φ	$0.2\ rad$

TABLE I: Parameter Test 1 and 4

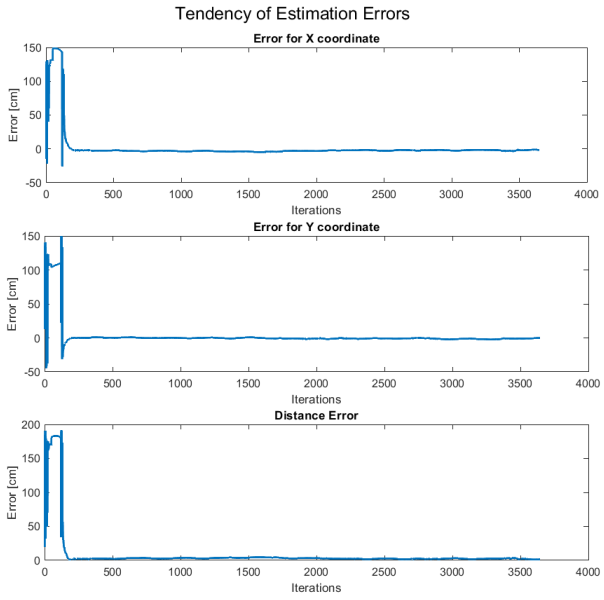

Fig. 1: Test 1: Tendency of estimation errors of tag x coordinate position, y coordinate position and total error distance

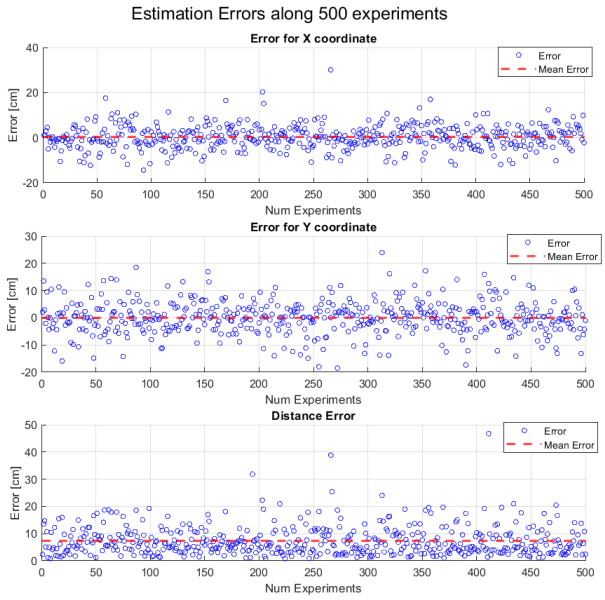

Fig. 2: Test 1: Mean errors in x and y coordinate and total distance along 500 experiments

B. Analysis with different encoder errors

In Fig. 3 are reported the results of a Monte-Carlo simulation performed with the different values of constants K_R,K_L, associated to different circumstances of encoder accuracy, as shown in Table II.

The results prove the fact that the algorithm implemented, it represents an unbiased estimator with zero mean, both for x and y coordinate.

As expected, the variance of each test increased as the encoder's error increased. A similar analysis may be performed for the overall distance error of the tag estimation: as the

Cases	K_R, K_L
Case 1	$0.01\,10^-2$
Case 2	$0.01\,10^-3$
Case 3	$0.01\,10^-4$

TABLE II: Parameter Test 2: Constant parameters used for variance value of the encoders error

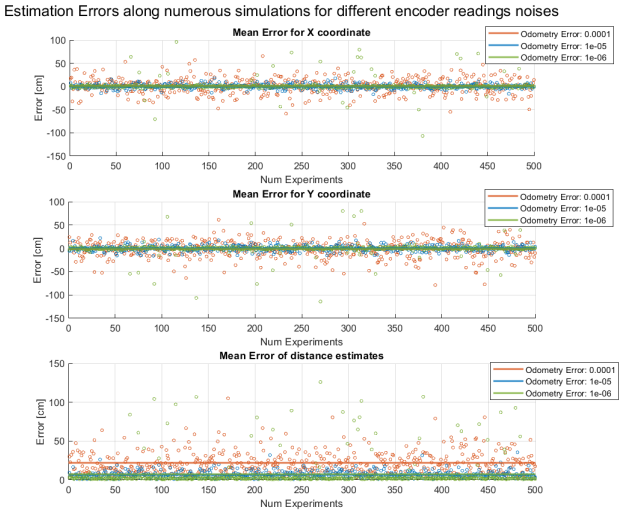

Fig. 3: Test 2: Mean errors along 500 experiments with different encoder errors condition

odometry error grows, so does the error on the distance.

C. Analysis with different phase measurement errors

Cases	σ_φ
Case 1	0.2 rad
Case 2	$\pi/4$ rad
Case 3	$\pi/2$ rad
Case 4	$3/4 \cdot \pi$ rad
Case 5	π rad
Case 6	2π rad

TABLE III: Parameter Test 3: Standard deviations used in different test case for phase measurement sensitivity analysis

The goal of this experiment was to test different scenarios regarding the accuracy of the sensor that measures the phase, in order to understand how much the noise on the phase measurements affects the estimate. This effect is described by the standard deviation of the measurement's noise. Table III reports the different values of the standard deviation have been used.

The results of a Monte-Carlo simulation with standard deviations less than $\pi/2$ rad are shown in Fig.4. Similar to the considerations in Section V-B, increasing the variation of the phase measurement error results in lower precision in the tag estimation location.

The same experiment has been performed for values of standard deviations bigger than $\pi/2$, as shows Fig. 5. In this figure it is possible to notice an interesting outcome: independently from the value of the noise the estimate error

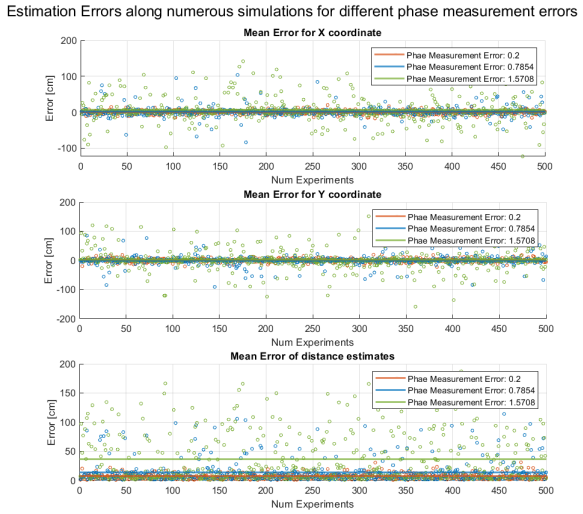

Fig. 4: Test 3a: Mean errors along 500 experiments with phase error standard deviation values of 0.2, $\pi/4$, $pi/2$ rad

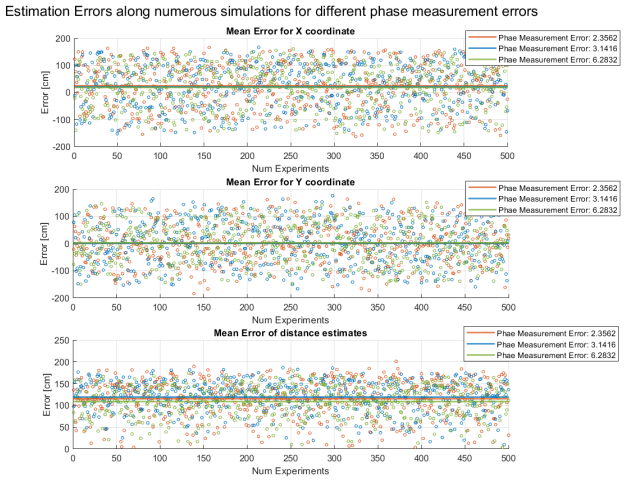

Fig. 5: Test 3b: Mean errors along 500 experiments with phase error standard deviation values of $3/4\,\pi$, π, 2π rad

stays stable around $1 - 1.5m$, which is actually a very bad estimate, while for the previous cases (Fig.4), the estimate error was close to zero for low values of noise and it changed in an understandable way based on the variation of noise and the variances are also quite bad, resulting in estimates that are spread all over the range. On the other hand, for the previous cases (Fig.4), the estimate error was close to zero for low values of noise and it changed in an understandable way based on the change in noise.

It is clear that the algorithm performs poorly in circumstances when σ_φ is greater than $\pi/2$. This suggests that an RFID system with a noise's standard deviation of $\pi/2$ could be regarded as the critical threshold for a functional estimation algorithm.

D. Analysis of the distributed algorithm

As previously mentioned, the second part of the project focused on implementing a distributed algorithm in order to

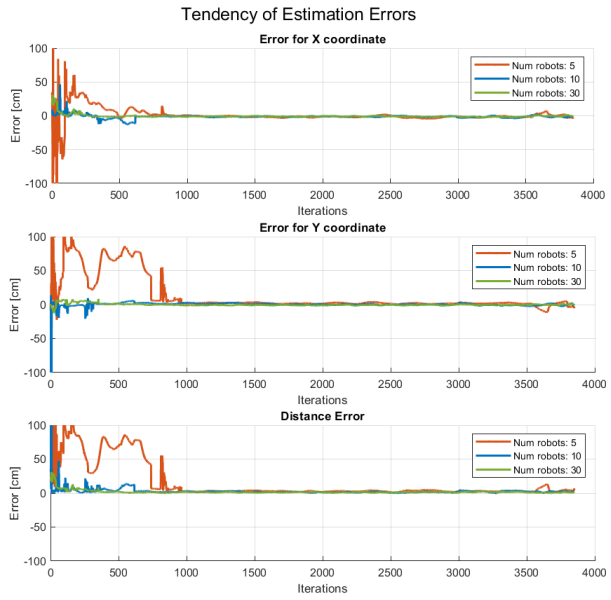

Fig. 6: Test 4: Tendency of estimation errors x and y coordinate of tag position and total error distance

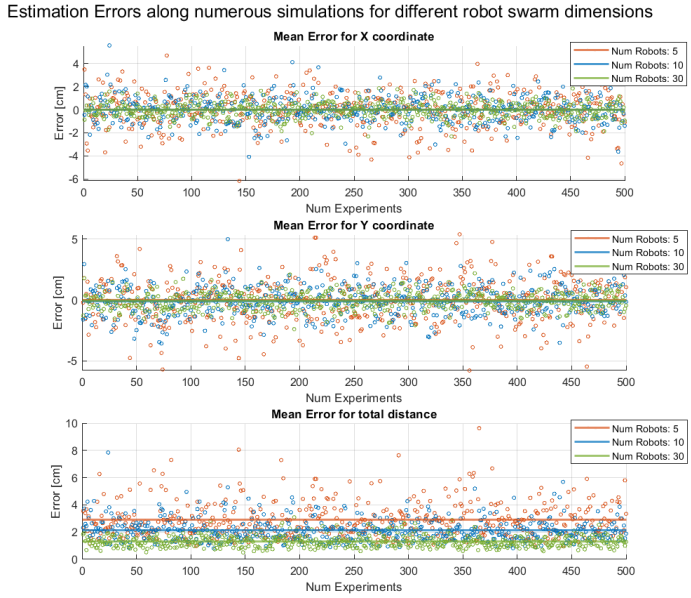

Fig. 7: Test 4: Mean errors along 500 experiments with swarm dimension of 5, 10, 30 robots

obtain a better estimate of the tag's position than what could be obtained with a single robot, which was already demonstrated to be good in the previous sections.

The behaviour of the distributed algorithm was analysed with different swarm sizes. The number of robots used in every case is reported in Table IV, while the parameters regarding the measurements noises are shown in Table I.

For each scenario, the outcomes of a single experiment are displayed in Fig. 6. It is possible to observe that more robots are present in the swarm and faster is the convergence to zero of the estimation error.

Similar to the other tests, Fig. 7 displays the outcomes of

Cases	Swarm dimension
Case 1	5 robots
Case 2	10 robots
Case 3	30 robots

TABLE IV: Parameter Test 4: Number of robots used in the distributed system tests

a Monte Carlo simulation conducted across 500 experiments. It has been demonstrated that also this approach can provide an unbiased estimator, and it demonstrates the quality of the algorithm, which produces an estimating error of less than 3 cm, on average, with a minimum of 5 robots. This signifies that the result in Section V-A has been improved by at least 50%.

VI. Conclusions

The primary goal of this project was to design an algorithm for tag localization using RFID technology. The key issue of this strategy was to come up with a solution to the phase ambiguity problem, while also obtaining the most precise estimate of the RFID tag's position.

This difficulty was successfully met by implementing multiple Kalman filters, evaluated across various initial conditions.

We next used a distributed approach to improve the precision of our estimates.

The achieved results were notably promising, particularly when considering the practical application envisioned. We contemplate employing this search algorithm for locating items, such as crates, within a warehouse setting. Overall, we are pleased with the outcomes and anticipate further exploration of this methodology in related applications.

Our simulations primarily aimed at validating the efficacy of the tag-searching algorithm, prompting the creation of a straightforward environment for testing. While our current analysis serves its purpose, a more comprehensive examination could consider aspects that closely mirror real-world scenarios. As a matter of fact, phase measurements are typically influenced by various factors such as signal multipath, fixed offsets, and other parameters, leading to the formulation $\hat{\varphi} = \varphi + \varphi_{\text{off}} + \varphi_m + \eta_\varphi$, differently from the model we used where we considered only a Gaussian noise.

Another important consideration is that in our experiments,the robots could roam freely inside the environment because no collision avoidance method was implemented in the simulation.

We utilised a planar study example for simplicity, but the algorithm can be expanded to identify the tag in three-dimensional space.

Nonetheless, this study proves the system's capacity to recognise the tag even when the robot's estimated location is only based on odometry. In terms of cost, this is an important result that demonstrates that a good estimate may be obtained with a less expensive sensor configuration. However, future improvements could involve the incorporation of an external positioning system, which would produce better results.

Additionally, the navigation scheme employed by the robots for tag localization within the room is not optimized. Introducing algorithms for environmental analysis could enhance the efficiency of the tag search process.

As stated in Section I, the distributed strategy was adopted to improve the algorithm's efficacy and precision. As shown in Fig. 7, this goal was met, and it also demonstrates that increasing the number of robots in the swarm improves the precision and accuracy of the tag location estimation. Of course, the test we ran represented an ideal circumstance in which the number of robots is unlimited, however in real-world applications, we would not have access to such a large number of robots for cost and feasibility reasons.

Clearly, this is a preliminary result and future improvements could better consider real-world factors, navigation optimization, and explore cost-effective sensor configurations. Nevertheless, our RFID-based algorithm successfully addressed tag localization challenges using multiple Kalman filters and a distributed approach, revealing some interesting potential behind the adopted technique.

VII. Appendix

Here are reported the complete derivation of matrices F and W, the Jacobians matrices of the filter state dynamics:

$$F_k = \begin{pmatrix} 1 & \hat{u}_k \sin(\hat{\beta}_k) & 0 & 0 & 0 \\ -\frac{\hat{u}_k}{\hat{\rho}_k^2} \sin(\hat{\beta}_k) & 1 + \frac{\hat{u}_k}{\hat{\rho}_k} \cos(\hat{\beta}_k) & 0 & 0 & 0 \\ 0 & 0 & 1 & 0 & -\hat{u}_k \sin\hat{\theta}_k \\ 0 & 0 & 0 & 1 & \hat{u}_k \cos\hat{\theta}_k \\ 0 & 0 & 0 & 0 & 1 \end{pmatrix}$$

$$W_k = \begin{pmatrix} -\frac{1}{2}\cos\hat{\beta}_k & -\frac{1}{2}\cos\hat{\beta}_k \\ \frac{1}{d} + \frac{1}{2\hat{\rho}_k}\sin(\hat{\beta}_k) & \frac{1}{d} + \frac{1}{2\hat{\rho}_k}\sin(\hat{\beta}_k) \\ \frac{1}{2}cos(\hat{\theta}_k) & \frac{1}{2}cos(\hat{\theta}_k) \\ \frac{1}{2}sin(\hat{\theta}_k) & \frac{1}{2}cos(\hat{\theta}_k) \\ \frac{1}{d} & -\frac{1}{d} \end{pmatrix}$$

References

[1] R. Miesen et al., "Where is the tag?" IEEE Microw. Mag., vol. 12, no. 7, pp. S49–S63, Dec. 2011.

[2] E. DiGiampaolo and F. Martinelli, "An algorithm for automatic grasping an UHF RFID passive tag" in 2020 IOP Conf. Ser.: Mater. Sci. Eng. 922 012010

[3] E. DiGiampaolo and F. Martinelli, "Range and Bearing Estimation of an UHF-RFID Tag Using the Phase of the Backscattered Signal," in IEEE Journal of Radio Frequency Identification, vol. 4, no. 4, pp. 332-342, Dec. 2020, doi: 10.1109/JRFID.2020.3016168.

The authors have the following addresses: Italy elia.bontempelli, alessandro.rizzardi@studenti.unitn.it.

This report is the final document for the course of "Distributed Systems for Measurement and Automation".